Hindawi
Geofluids
Volume 2021, Article ID 6695975, 9 pages
https://doi.org/10.1155/2021/6695975

Research Article

Static and Dynamic Mechanical Properties of Organic-Rich Gas Shale

Hui Li,[1] **Chi Dong**,[2] **Hongwei Yu**,[3] **Xin Zhao**,[3] **Yan Li**,[4] **Lele Cao**,[1] **and Ming Qu**[1]

[1]*China University of Petroleum, Beijing, China*
[2]*Northeast Petroleum University, Daqing, China*
[3]*Research Institute of Petroleum Exploration & Development, Beijing, China*
[4]*Institute of Mineral Resources Research, China Metallurgical Geology Bureau, Beijing, China*

Correspondence should be addressed to Hui Li; 20234914@qq.com

Received 15 October 2020; Revised 1 December 2020; Accepted 25 March 2021; Published 13 April 2021

Academic Editor: Tao Chen

Rock mechanical properties are critical for drilling, wellbore stability, and well stimulation. There are usually two laboratory methods to determine rock mechanical properties: static compression tests and acoustic velocity measurements. Rocks are heterogeneous, so there are significant differences between static elastic constants and the corresponding dynamic ones. Usually, static test results are more representative than dynamic methods but the static tests are time consuming and costly. Dynamic methods are nondestructive and less expensive, which are practical in the laboratory and field. In this paper, we compare the static and dynamic elastic properties of Eagle Ford Shale by triaxial compressive tests and ultrasonic velocity tests. Correlations between static and dynamic elastic properties are developed. Conversion from dynamic mechanical properties to static mechanical properties is established for better estimating reservoir mechanical properties. To better understand the relationship of static and dynamic mechanical properties, 30 Eagle Ford Shale samples were tested. According to the test results, the dynamic properties are considerably different from the static counterparts. For all tested samples, static Young's modulus is lower than dynamic Young's modulus, ranging from 55% to 90%. The difference of the static and dynamic Young's moduli decreases with the increasing of confining pressure. The reason may be because the microcracks closed in high confining pressure. Correlations between static and dynamic Young's modulus are developed by regression analysis, which are crucial to understand the rock mechanical properties and forecast reservoir performance when direct measurement of static mechanical properties is not available or expensive. There are no strong correlations between static and dynamic Poisson's ratios observed for the tested samples. Two potentially major reasons for the discrepancy of the static and dynamic properties of Eagle Ford Shale are discussed. Lithology and heterogeneity may be the inherent reasons, and external causes are probably the difference in strain amplitude and frequency.

1. Introduction

In recent decades, shale gas is more and more important in the global energy and petroleum industry. Shale gas in the U.S.A. is predicted (AEO, 2011) at about 45% of all gas production by 2035. The increasing significance of shale gas reservoirs needs deeper understanding of shale behaviors. Most shale rocks are heterogeneous and anisotropic, which contain quartz, clays, carbonates, feldspars, and so on. Knowledge of mechanical properties of shale rocks is important in lost return, wellbore stability, and hydraulic fracturing design during shale gas development [1, 2]. The most widely used mechanical properties in oil development are Young's modulus and Poisson's ratio, which affect the fracture growth during hydraulic fracturing [3, 4]. Mechanical properties can be obtained either from static compression tests or from dynamic acoustic velocity measurements [5]. Determining rock static elastic properties directly from compression tests is time consuming, complicated, and expensive. While determining dynamic elastic properties in the laboratory as well as in in situ condition is easy, nondestructive, and inexpensive. Therefore, prediction of static elastic properties from

dynamic elastic parameters and investigation of the correlations of rock static and dynamic properties are meaningful and necessary. The laboratory measurements of rock mechanical properties include ultrasonic velocity tests from which the dynamic elastic parameter can be determined as well as direct strength tests including compressive tests and tensile tests, where rock strength and static elastic properties are determined.

Many studies have worked on establishing the relationships between static and dynamic elastic properties of limestones, sandstones, carbonate, and granites [6–13]. Ide [14] first indicated that dynamic Young's modulus is higher than static Young's modulus for granite samples. Simmons and Brace [15] concluded that the dynamic elastic modulus was considerably higher than static elastic modulus when confining pressure is low. The difference was decreased when confining pressure increased. When confining pressure is in excess of 30,000 psi, the static and dynamic moduli are closely equal to each other. King's [16] experimental results indicated that dynamic modulus was always higher than static modulus of Boise sandstones. Jizba and Nur [17] conducted a simultaneous experiment to investigate the static and dynamic bulk moduli on sandstones. They concluded that the static and dynamic bulk moduli were linear related and the correlation was affected by confining pressure. Yale and Jamieson [18] concluded that static elastic constants and dynamic elastic constants are different for most rocks. Testing frequency and pore fluid may cause the differences. Ciccitti and Mulargia [19] concluded that the static modulus of Calcare Massiccio mudstone-limestone is 5–10% lower than the dynamic modulus. Holt et al. [20] conducted an experiment on three different shales and concluded that dynamic moduli are higher than the static counterparts. And the difference was related to inclination angle. He et al. [9] proposed that the dynamic moduli of Bakken samples were considerably different from the static moduli measured by triaxial compression tests.

Previous research on the comparison of static and dynamic properties mainly focuses on sandstone, limestone, and carbonate [6, 17, 21, 22]. In this paper, we focus on measuring and comparing the static and dynamic elastic properties of Eagle Ford Shale. Static elastic properties were measured by triaxial compression tests. Ultrasonic velocity measurements were conducted to obtain the dynamic elastic properties with 1 MHz frequency. Correlations are developed based on the static and dynamic parameters of 30 Eagle Ford Shale samples to adjust the uncertainty of elastic moduli calculated from the acoustic measurements for Eagle Ford Shale formation and to lower the cost and test time.

2. Theory and Experimental Procedures

2.1. Theory. According to Hook's law, the static mechanical properties investigated in this work are static Young's modulus (E_s) and static Poisson's ratio (ν_s) which are the key parameters to determine rock mechanical properties. In this study, static Young's modulus (E_s) and static Poisson's ratio (ν_s) are measured from triaxial compression tests. Static Young's modulus is calculated as equation (1):

$$E_s = \frac{\Delta\sigma}{\Delta\varepsilon}, \tag{1}$$

where σ is the axial stress and ε is the axial strain.

The static Poisson's ratio is expressed as equation (2):

$$\nu_s = \left|\frac{\varepsilon_y}{\varepsilon_x}\right|, \tag{2}$$

where ε_y is lateral strain ε_y and ε_x is the longitudinal strain.

Dynamic Young's modulus (E_d) and dynamic Poisson's ratio (ν_d) can be calculated from acoustic velocities and sample bulk density. The elastic constants are calculated based on equations (3) and (4) (Brich, 1960, and Kate, 2012).

$$E_d = \rho v_s^2 \left(\frac{3v_p^2 - 4v_s^2}{v_p^2 - v_s^2}\right), \tag{3}$$

$$\nu_d = \frac{v_p^2 - 2v_s^2}{2\left(v_p^2 - v_s^2\right)}, \tag{4}$$

where ρ is sample density, g/cm^2, v_p is compressional wave velocity, and v_s is shear wave velocity, km/s.

2.2. Sample Descriptions. In this work, Eagle Ford Shale samples were used to investigate the relationship between static elastic properties and dynamic counterparts. All the tested samples are prescreened for visible microcracks using a computed tomography (CT) scanner with a resolution of 30 μm, and only these samples with no recognizable fractures are used for testing. Eagle Ford Shale is dark colored calcareous mudstone with small amounts of clay minerals. White stringers of calcite with thickness about 1 mm or less are obvious on the end faces of the sample plugs (Figure 1). The SEM photomicrograph (Figure 2) shows the calcite microcrystalline crystals and grains, the nanofossil fragments, and organic matter filling the pore space. The TOC ranges from 2.1 wt% to 5.9 wt%, likely resulting in the dark color. X-ray diffraction (XRD) data shows the average of 24.2% quartz, 62.2% calcite, and 5.5% of total clays, with minor amounts of dolomite, gypsum, and pyrite.

2.3. Experimental Procedures. 30 cylindrical Eagle Ford Shale samples were prepared for this study with 1 inch in diameter and 3 inches in length. Each sample was cut into two subsamples. Subsample A is 2 inches in length, which is used for the triaxial compression test. Subsample B is 1 inch in length, which is for the acoustic velocity test. Because the two subsamples are cut from one sample, we regard that heterogeneity is not the dominant reason that caused the difference of the test results. Then, the triaxial compressive tests and acoustic velocity tests were conducted on each subsample at room temperature (20°C). The sample preparation and test procedures strictly followed the ASTM standard. Triaxial compression strength, static Young's modulus, and static Poisson's ratio were obtained from subsample A. Dynamic

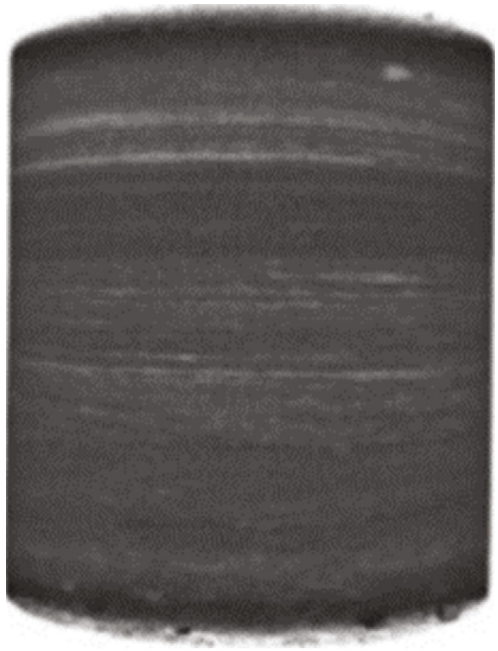

Figure 1: CT radiograph of an Eagle Ford sample cored perpendicular to bedding.

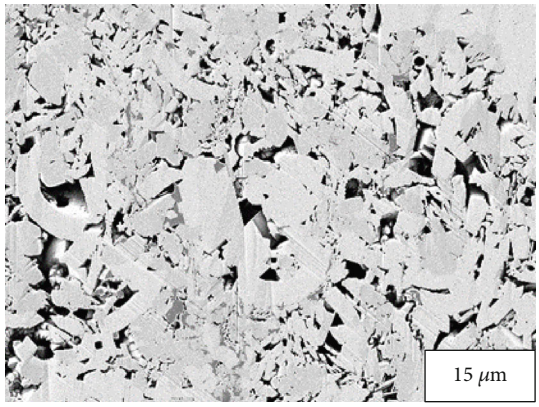

Figure 2: SEM photomicrograph of an Eagle Ford sample cored parallel to bedding.

Young's modulus and dynamic Poisson's ratio were determined from subsample B. The experimental setup schematics of acoustic velocity tests and triaxial compressive tests are shown in Figures 3 and 4.

Before triaxial compression tests and ultrasonic velocity tests, samples were prescreened using an industrial CT with a resolution of 30 μm; only the samples without detectable fractures were used in the tests. All samples were dried for 24 hours, and then, physical parameters were measured before static and dynamic tests. Triaxial compression tests were performed on each subsample A. Displacement control was used to conduct the compression test and loading rate was based on the ASTM standard (ASTM D3967-08) [23]. Acoustic velocity measurements were performed on each subsample B following the ASTM D2845 [24] standard at various confining pressures (4, 7, 14, 20, 27, and 35 MPa) with 1 MHz frequency acoustic velocity sensors in all tests.

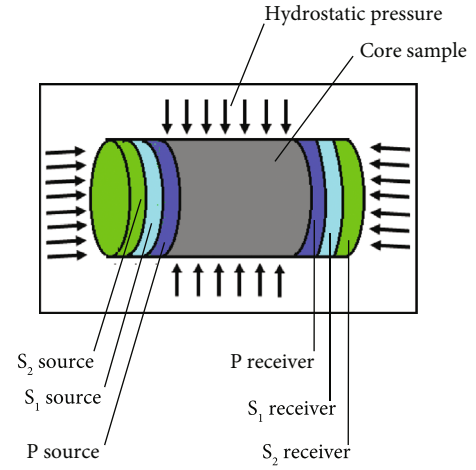

Figure 3: The experimental setup schematic of acoustic velocity tests.

The reason why we choose these confining pressures is based on the formation pressure under a normal pressure system. After mechanical tests, samples were crushed to measure the mineralogy and TOC. Then, static and dynamic elastic constants were determined from the results of triaxial compression tests and acoustic velocity tests, respectively.

3. Experimental Results and Analysis

Triaxial compression tests and acoustic velocity tests were conducted on 30 Eagle Ford Shale samples. Static and dynamic elastic constants were obtained according to equations (1) to (4). Relations between static and dynamic parameters were investigated by regression analysis. The correlations of static and dynamic elastic constants were discussed below.

3.1. V_p and V_s Relationships. The linear relationship of V_p and V_s was observed (Figure 5). As shown in Figure 5, V_p and V_s are very well correlated with high regression coefficient, $R^2 = 0.91$; the correlation equation of V_p and V_s is shown in equation (5). The V_s can be well predicted in the same formation. Because the acquisition of V_p from seismic data is much cheaper than V_s, this correlation equation is valuable for estimating V_s from V_p.

$$V_s = 0.4502V_p + 0.6214. \quad (5)$$

3.2. Correlation between Static and Dynamic Young's Moduli. After triaxial compression tests and ultrasonic velocity tests, as well as according to equations (1) and (4), static and dynamic Young's moduli were obtained and compared with various confining pressure (4, 7, 14, 20, 27, and 35 MPa); see Figures 6–11. In the tested Eagle Ford Shale samples, static and dynamic Young's moduli are linearly correlated and static Young's moduli are always lower than the dynamic Young's moduli under all tested confining pressure. Our test

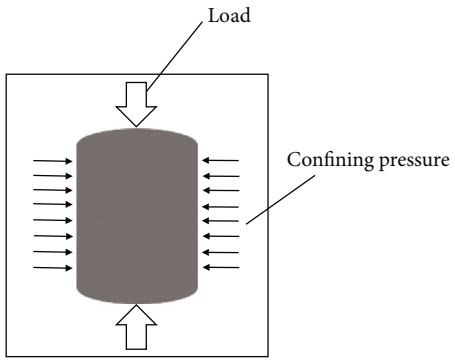

Figure 4: The experimental setup schematic of triaxial compressional tests.

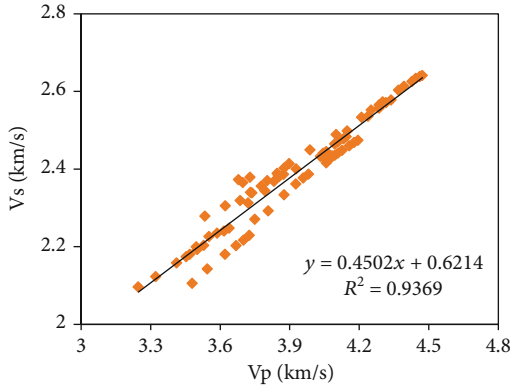

Figure 5: V_p and V_s relationship of the tested Eagle Ford samples.

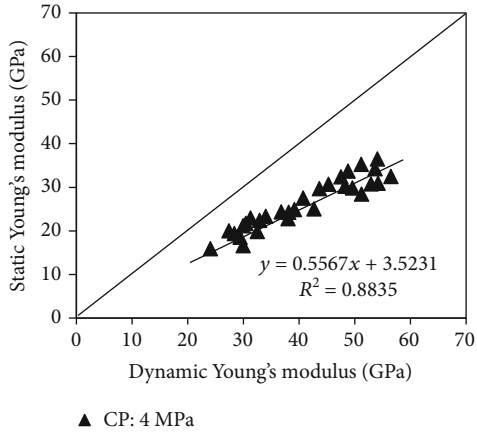

Figure 6: Correlation between E_s and E_d when CP is 4 MPa.

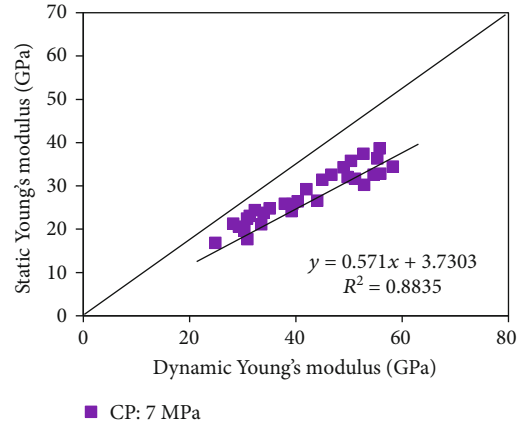

Figure 7: Correlation between E_s and E_d when CP is 7 MPa.

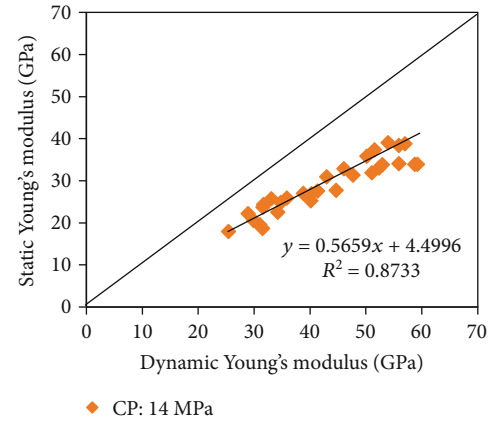

Figure 8: Correlation between E_s and E_d when CP is 14 MPa.

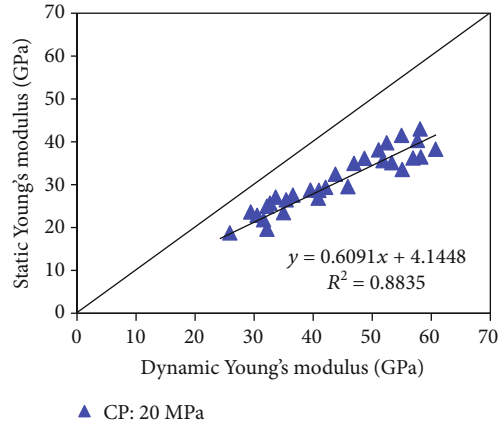

Figure 9: Correlation between E_s and E_d when CP is 20 MPa.

results are consistent with most of the previous studies [15, 19, 20].

Figure 12 showed the relation between static and dynamic Young's moduli under different confining pressures. As confining pressure increased from 4 MPa to 35 MPa, the trendline of static and dynamic Young's moduli is gradually close to the 45° straight line, indicating the difference is static and dynamic Young's moduli which decreased with confining pressure increase. The correlations of static and dynamic Young's moduli under various confining pressures are listed in Table 1. As observed, the static and dynamic Young's moduli have good linear correlation with coefficient of correlation between 86% and 88%. With the confining pressure increasing from 4 MPa to 35 MPa, the difference of maximum dynamic Young's moduli and maximum static Young's moduli decreased, from 24.03 GPa to 18.41 GPa. The ratio of static Young's moduli to dynamic Young's moduli also verified the difference of the static and

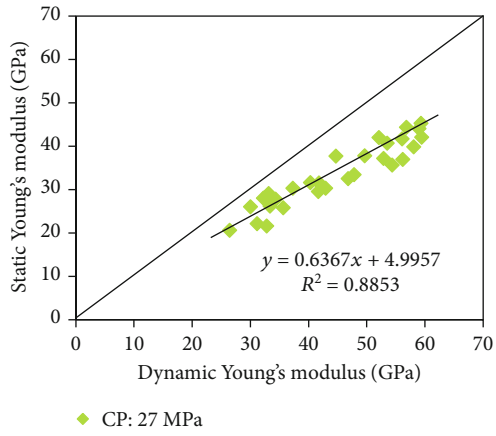

Figure 10: Correlation between E_s and E_d when CP is 27 MPa.

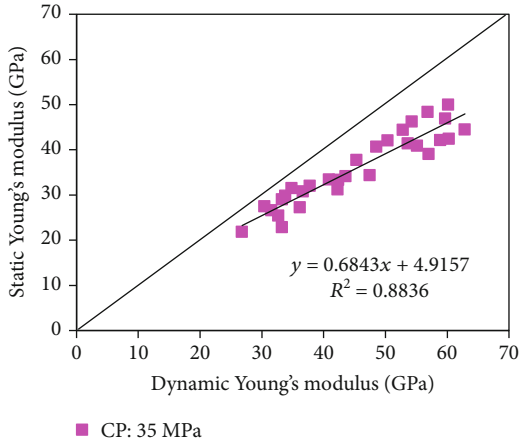

Figure 11: Correlation between E_s and E_d when CP is 35 MPa.

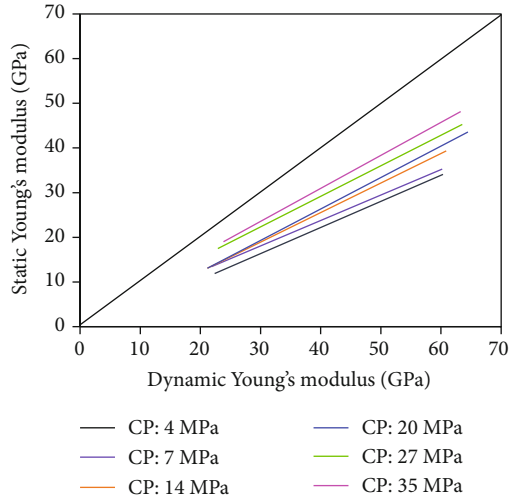

Figure 12: Correlation between E_s and E_d with various confining pressure.

dynamic Young's moduli which decreases with the increasing of confining pressure, which is consistent with previous studies [17, 25]. The reason may because the microcracks closed in high confining pressure.

Table 1: Correlations between E_s and E_d.

CP (MPa)	Correlation	R^2	max $(E_d - E_s)$ (GPa)	E_s/E_d
4	$E_s = 0.5567E_d + 3.5231$	0.8635	24.03	55%–74%
7	$E_s = 0.571E_d + 3.7303$	0.8721	23.94	57%–76%
14	$E_s = 0.5836E_d + 3.967$	0.8718	23.36	59%–77%
20	$E_s = 0.6091E_d + 4.1448$	0.8835	22.56	62%–80%
27	$E_s = 0.6367E_d + 4.9957$	0.8803	19.32	65%–88%
34	$E_s = 0.6843E_d + 4.9157$	0.8836	18.41	68%–90%

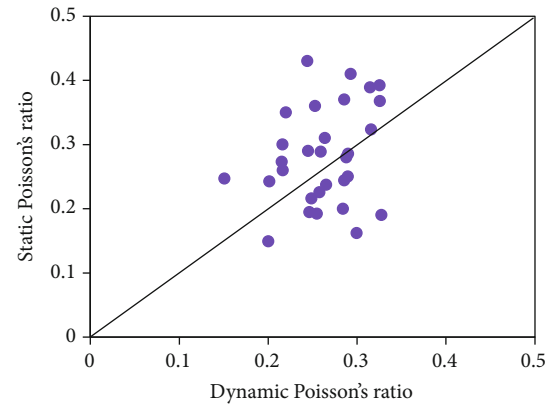

Figure 13: Correlation between static and dynamic Poisson's ratios when confining pressure is 20 MPa.

3.3. Static and Dynamic Poisson's Ratios. The correlation between static and dynamic Poisson's ratios is not distinct. Unlike Young's modulus, the relationship between static and dynamic Poisson's ratios is significantly scattered. Figure 13 exhibited the static and dynamic Poisson's ratios when confining pressure is 20 MPa. As observed, the data points are quite discrete and less consistent. There are also no correlations between the static and dynamic Poisson's ratios under other confining pressures (4, 7, 14, 27, and 35 MPa). The reason why the correlation between dynamic and static Poisson's ratios is poor may partially be because of the heterogeneous and anisotropic properties of Eagle Ford shale. The existence of microcrack and hard minerals in the sample may also cause the scatter of the correlation.

3.4. Validating the Proposed Correlations. According to the correlations between static and dynamic Young's moduli under various confining pressure (Table 1), the static Young's modulus can be estimated by dynamic Young's modulus, which is named as predicted static Young's modulus (E_{sp}). To verify the validity of the empirical relations, the predicted static Young's modulus have been compared with the measured static Young's modulus (E_{sm}). Figures 14–19 showed the predicted static Young's modulus versus the

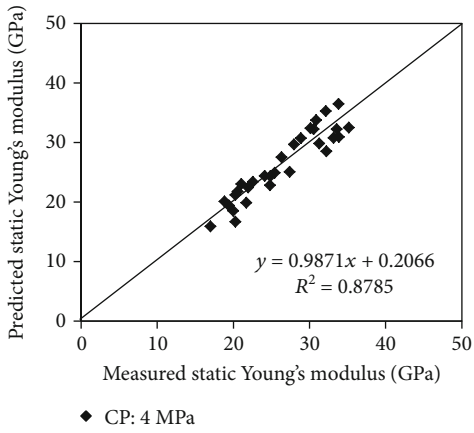

Figure 14: Correlation between E_{sp} and E_{sm} when CP is 4 MPa.

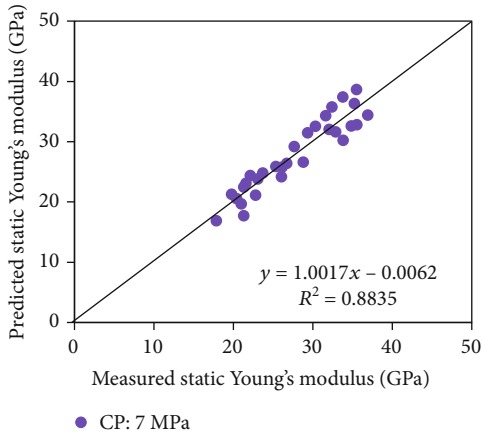

Figure 15: Correlation between E_{sp} and E_{sm} when CP is 7 MPa.

measured static Young's modulus under different confining pressures. As observed, both E_{sp} and E_{sm} distribute close to the 45° straight line, which means dynamic Young's modulus is reliable to estimate static Young's modulus for the tested Eagle Ford Shale. Table 2 illustrated the linear correlations between E_{sp} and E_{sm} under various confining pressures. The regression coefficients are high, which are between 86% and 88%.

4. Discussions

It is necessary to investigate the causes of the difference between static and dynamic parameters, which have been studied for decades on various rocks, including sandstones, chalks, and carbonates. However, to quantify the causes for shale still remains challenging. Two potentially major reasons are inherent causes and external causes.

4.1. Inherent Causes. Porosity and pore fluid may be the inherent reasons to cause the discrepancy between the static and dynamic properties [9, 26, 27]. The pore fluid is an important factor of the difference between the static and dynamic properties even in partially saturated rocks, and it has been argued that the difference between the static and dynamic moduli can be corrected using Biot's theory [28].

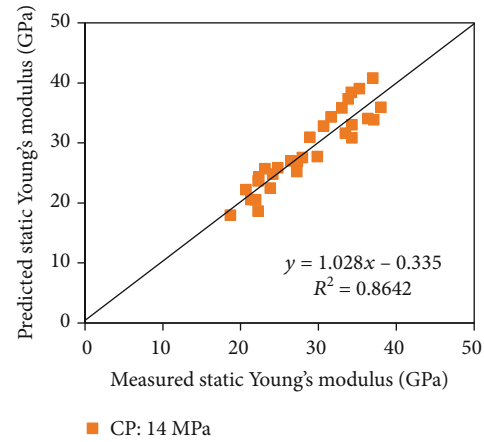

Figure 16: Correlation between E_{sp} and E_{sm} when CP is 14 MPa.

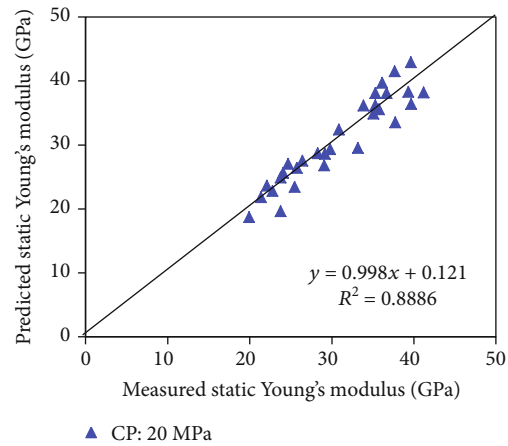

Figure 17: Correlation between E_{sp} and E_{sm} when CP is 20 MPa.

However, even in carefully dried rocks there is a significant difference between the static and dynamic moduli [16]. In this study, porosity and pore fluid cannot be the key factors for the difference between the static and dynamic properties of Eagle Ford Shale samples. Figure 20 illustrated the porosity of the tested 30 Eagle Ford samples. As observed, the porosity of the tested samples is small and most of the values are between 4% and 6% and all the tested Eagle Ford samples are in air-dried condition. The porosity and pore fluid may not be the dominant factors. Lithology and heterogeneity may be the inherent reasons for the discrepancy between the static and dynamic properties of Eagle Ford Shale. The dynamic and static elastic parameters are nearly equal for homogeneous materials. Previous studies have already verified that Eagle Ford Shale is heterogeneous and anisotropic [1, 29]. The heterogeneity and anisotropy of Eagle Ford Shale may cause the difference between the dynamic mechanical properties and the static mechanical properties.

4.2. External Causes. The difference between static and dynamic parameters are related to the differences in the strain amplitude and frequency between the two measurements. The static test exerts large strain amplitude (10^{-5}–

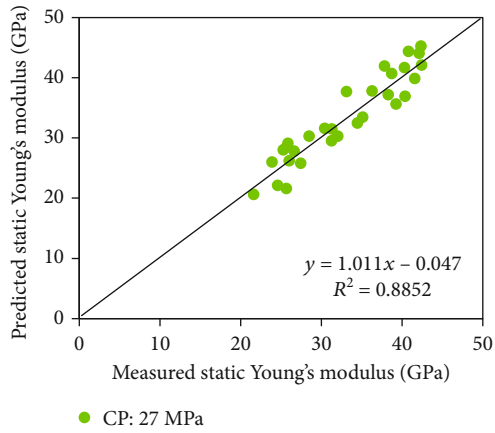

Figure 18: Correlation between E_{sp} and E_{sm} when CP is 27 MPa.

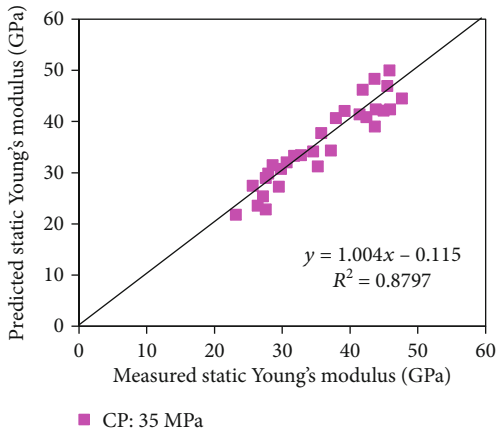

Figure 19: Correlation between E_{sp} and E_{sm} when CP is 35 MPa.

Table 2: Correlations between predicted E_s and measured E_s.

CP (MPa)	Correlation	R^2
4	$E_{sp} = 0.967E_{sm} + 0.206$	0.8705
7	$E_{sp} = 1.071E_{sm} - 0.062$	0.8835
14	$E_{sp} = 1.028E_{sm} - 0.335$	0.8624
20	$E_{sp} = 0.998E_{sm} + 0.121$	0.8885
27	$E_{sp} = 1.011E_{sm} - 0.047$	0.8852
34	$E_{sp} = 1.004E_{sm} - 0.115$	0.8797

10^{-3}), while the order of the dynamic test amplitude is 10^{-6} [30]. It is probably impossible to accurately measure static parameters at acoustic strain amplitude. Larger static strain amplitude results in a friction sliding along the crack surface or boundary of grains and then softens the rock which could decrease the static moduli [7, 30]. The dynamic strain amplitude is too small to induce this kind of friction sliding, and the dynamic strain amplitude has little impact on the dynamic moduli [31, 32]. Meanwhile, dynamic measurement applies high frequency (10^4–10^5 Hz), which could harden the rock and increase the dynamic moduli. While the low frequency (10^{-4}–10^{-1} Hz) of static test could cause the viscoelastic deformation, which would not occur in the high-frequency acoustic test [18]. Other reasons like sample scale effect and loading eccentricity may partially contribute to the discrepancy of the static and dynamic parameters. In this paper, we performed the triaxial compression measurements with 10^{-4} Hz strain amplitude and 0.5 Hz frequency, while the ultrasonic velocity test with 10^{-6} Hz strain amplitude oscillation and 1 MHz frequency. The discrepancy of the strain amplitude and frequency between the two kinds of measurements is the dominant external causes. Other factors may also contribute to the difference of the dynamic and static properties, including scale effects of the testing samples, test performing conditions, and site circumstances.

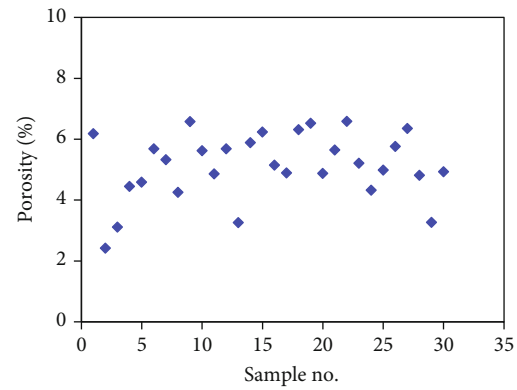

Figure 20: Porosity of the tested Eagle Ford Shale samples.

5. Conclusions

In this paper, the comparison of the static and dynamic mechanical properties was conducted on 30 Eagle Ford Shale samples. The correlations between the static and dynamic mechanical properties were developed. The specific conclusions are as follows:

(1) V_p and V_s are very well correlated with high regression coefficient. The correlation equation of V_p and V_s is developed and V_s can be well predicted by V_p

(2) The dynamic Young's modulus of Eagle Ford Shale is considerably different from the static counterpart. For all tested samples, static Young's modulus is lower than dynamic Young's modulus, ranging from 55% to 90%. Correlations between the static and dynamic Young's moduli are developed by regression analysis

(3) The difference between the static and dynamic Young's moduli decreases with the increasing of confining pressure. The reason may be because the microcracks closed in high confining pressure

(4) There is no strong correlation between the static and dynamic Poisson's ratios observed for the tested Eagle Ford samples

(5) Two potentially major reasons for the discrepancy of the static and dynamic properties of Eagle Ford Shale are discussed. Lithology and heterogeneity may be the inherent reasons, and external causes are probably the difference of strain amplitude and frequency

Data Availability

The data used to support the findings of this study are included within the article.

Conflicts of Interest

The authors declare that they have no conflicts of interest.

Authors' Contributions

Hui Li did the conceptualization, methodology, and formal analysis; Chi Dong did the grammar and language checking and editing; Hongwei Yu did the investigation, writing, reviewing, and editing; Xin Zhao did the investigation and formal analysis; Yan Li did the writing, reviewing, and editing; Lele Cao did the data curation, writing, and original draft preparation; and Ming Qu did the writing, reviewing, and editing.

Acknowledgments

This research was supported by the National Science Foundation of China (no. 51834005), by the Major Project of China National Petroleum Corporation (2018E-1805), by the Innovation Fund of China National Petroleum Corporation (2019D-5007-0201), and by the Science Foundation of China University of Petroleum, Beijing (no. 2462020XKBH013).

References

[1] H. Li, B. T. Lai, S. Y. Qin et al., "The effects of water content on transversely isotropic properties of organic rich gas shale," *Journal of Natural Gas Science and Engineering*, vol. 83, article 103574, 2020.

[2] Y. Li, M. Long, L. Zuo, W. Li, and W. Zhao, "Brittleness evaluation of coal based on statistical damage and energy evolution theory," *Journal of Petroleum Science and Engineering*, vol. 172, pp. 753–763, 2019.

[3] Y. Li, M. Long, J. Tang, M. Chen, and X. Fu, "A hydraulic fracture height mathematical model considering the influence of plastic region at fracture tip," *Petroleum Exploration and Development*, vol. 47, no. 1, pp. 184–195, 2020.

[4] J. Tang, K. Wu, L. Zuo, L. Xiao, S. Sun, and C. Ehlig-Economides, "Investigation of rupture and slip mechanisms of hydraulic fractures in multiple-layered formations," *SPE Journal*, vol. 24, no. 5, pp. 2292–2307, 2019.

[5] M. Ramulu and T. G. Sitharam, "Laboratory experiments for estimation of static and dynamic elastic modulus of jointed rock mass," *International Society for Rock Mechanics and Rock Engineering. ISRM-ARMS6-2010-031, ISRM International Symposium, 6th Asian Rock Mechanics Symposium*, 2010, New Delhi, India, October 2010, 2010.

[6] A. Bakhorji and D. R. Schmitt, "Laboratory measurements of static and dynamic bulk moduli in carbonate," in *ARMA-10-465 American Rock Mechanics Association 44th U.S. Rock Mechanics Symposium and 5th U.S.-Canada Rock Mechanics Symposium*, Salt Lake City, Utah, June 2010.

[7] E. Fjær, A. M. Stroisz, and R. M. Holt, "Static versus dynamic moduli: another piece in the puzzle," in *ARMA-2015-409, 49th U.S. Rock Mechanics/Geomechanics Symposium*, San Francisco, CA, USA, June-July 2015.

[8] M. Ghafoori, A. Rastegarnia, and G. R. Lashkaripour, "Estimation of static parameters based on dynamical and physical properties in limestone rocks," *Journal of African Earth Sciences*, vol. 137, no. 1, pp. 22–31, 2018.

[9] J. He, K. Ling, X. Wu, P. Pei, and H. Pu, "Static and dynamic elastic moduli of Bakken Formation," in *International Petroleum Technology Conference*, Beijing, China, March 2019.

[10] M. S. King, "Static and dynamic elastic properties of rocks from the Canadian Shield," *International Journal of Rock Mechanics and Mining Sciences & Geomechanics Abstracts*, vol. 20, no. 5, pp. 237–241, 1983.

[11] M. Karamia, B. Abrah, S. Dayani, L. Faramarzi, and M. G. Nik, "Empirical correlations between static and dynamic properties of intact rock," in *ISRM-ARMS7-2012-052. International Society for Rock Mechanics and Rock Engineering Source ISRM Regional Symposium -7th Asian Rock Mechanics Symposium*, Seoul, Korea, October 2012.

[12] I. Larsen, E. Fjær, and L. Renlie, "Static and dynamic Poisson's ratio of weak sandstones," in *American Rock Mechanics Association. 4th North American Rock Mechanics Symposium*, Seattle, WA, USA, July-August 2000.

[13] E. Yasar and Y. Erdogan, "Correlating sound velocity with the density, compressive strength and Young's modulus of carbonate rocks," *International Journal of Rock Mechanics and Mining Sciences*, vol. 41, no. 5, pp. 871–875, 2004.

[14] J. M. Ide, "Comparison of statically and dynamically determined Young's modulus of rocks," *Proceedings of the National Academy of Sciences of the United States of America*, vol. 22, no. 2, pp. 81–92, 1936.

[15] G. Simmons and W. F. Brace, "Comparison of static and dynamic measurements of compressibility of rocks," *Journal of Geophysical Research*, vol. 70, no. 22, pp. 5649–5656, 1965.

[16] M. S. King, "Static and dynamic elastic moduli of rocks under pressure," in *ARMA-69-0329, American Rock Mechanics Association. The 11th U.S. Symposium on Rock Mechanics*, Berkeley, CA, USA, June 1969.

[17] D. Jizba and A. Nur, "Static and dynamic moduli of tight gas sandstones and their relation to formation properties," in *SPWLA 31st Annual Logging Symposium*, Lafayette, LA, USA, June 1990.

[18] D. P. Yale and W. H. Jamieson, "Static and dynamic mechanical properties of carbonates," in *ARMA-1994-0463, American Rock Mechanics Association 1st North American Rock Mechanics Symposium*, Austin, TX, USA, June 1994.

[19] M. Ciccitti and F. Mulargia, "Differences between static and dynamic elastic moduli of a typical seismogenic rock," *Geophysical Journal International*, vol. 157, no. 1, pp. 474–477, 2004.

[20] R. M. Holt, O.-M. Nes, J. F. Stenebraten, and E. Fjaer, "Static vs. dynamic behavior of shale," in *46th U.S. Rock Mechanics/-Geomechanics Symposium*, Chicago, IL, USA, June 2012.

[21] A. Bilal, M. Myers, and L. Hathon, "An investigation of static and dynamic data using multistage tri-axial test," in *SEG Technical Program Expanded Abstracts 2016*, pp. 1–6, Society of Exploration Geophysicists, 2016.

[22] T. J. Plona and J. M. Cook, "Effects of stress cycles on static and dynamic Young's moduli in Castlegate sandstone," in *The 35th U.S. Symposium on Rock Mechanics*, Reno, NV, USA, June 1995.

[23] ASTM D3967-08, *Standard Test Method for Splitting Tensile Strength of Intact Rock Core Specimens*, American Society for Testing and Materials, 2008.

[24] ASTM D2845, *Standard Test Method for Laboratory Determination of Pulse Velocities and Ultrasonic Elastic Constants of Rock*, American Society for Testing and Materials, 1983.

[25] J. B. Walsh and W. F. Brace, "Elasticity of rock: a review of some recent theoretical studies," *Rock Mechanics and Engineering Geology*, vol. 4, p. 283, 1966.

[26] E. Fjaer, "Static and dynamic moduli of weak sandstones. American rock mechanics association Vail rocks," in *The 37th U.S. Symposium on Rock Mechanics*, Vail, CO, USA, June 1999.

[27] G. Hongkui, L. Yingsong, M. Shanzhou, and S. Lili, "Difference of rock elastic parameters under static and dynamic loading," in *ISRM-ARMS2-2001-011, International Society for Rock Mechanics and Rock Engineering. 2nd Asian Rock Mechanics Symposium*, Beijing, China, September 2001.

[28] H. Montmayeur and R. M. Graves, "Prediction of static elastic/mechanical properties of consolidated and unconsolidated sands from acoustic measurements: basic measurements," in *SPE 14159. SPE Annual Technical Conference and Exhibition*, Las Vegas, NV, USA, September 1985.

[29] B. T. Lai, H. Li, J. L. Zhang, D. Jacobi, and D. Georgi, "Water content effects on dynamic elastic properties of organic-rich shale," *SPE Journal*, vol. 21, no. 2, pp. 635–647, 2015.

[30] K. Winkler, A. Nur, and M. Gladwin, "Friction and seismic attenuation in rocks," *Nature*, vol. 277, no. 5697, pp. 528–531, 1979.

[31] A. Vachaparampil, L. Hu, X. Zhou, A. Ghassemi, I. Gill, and Y. Chitrala, "Geomechanical anisotropy of Utica Shale from static and dynamic measurements," in *ARMA-2016-046, 50th U.S. Rock Mechanics/Geomechanics Symposium*, Houston, TX, USA, June 2016.

[32] K. W. Winkler and A. Nur, "Seismic attenuation: effects of pore fluids and frictional-sliding," *Geophysics*, vol. 47, no. 1, pp. 1–15, 1982.